Systematic Study on the Application of Continuous Helical Blades for Assisting Extrusion of Multi-Materials

Huai-Chi Tsai* and Pei-Hsien Hsu

Graduate Institute of Architecture, National Yang Ming Chiao Tung University, Hsinchu, Taiwan, China
Email: jesuislameilleure@arch.nctu.edu.tw (H.-C.T.); phsu@arch.nycu.edu.tw (P.-H.H.)
*Corresponding author

Manuscript received May 31, 2023; revised August 11, 2023; accepted September 12, 2023; published May 28, 2024.

***Abstract*—This study explores the application of continuous helical blades in extrusion systems for multiple materials. To enhance the adaptability of extrusion systems to different material properties, the study divides the extrusion system into a main process and sub-branches, with the main process representing the components of the extrusion mechanism, and the variations in component parameters serving as the sub-branches. Once the final product design and chosen printing material are determined, the dimensions of the extrusion head (length, width, and height), as well as the spacing and angle of the continuous helical blades, can be determined. By utilizing Flow Simulation software for analysis, the system's discharge speed and frictional forces under different parameter combinations can be simulated, analyzed, and compared to identify the optimal configuration for specific conditions. This allows for the calculation of the required motor torque to complete the design of the extrusion system components. the objective of this research is to use the assistance of continuous helical blades to facilitate the extrusion process for various materials, ensuring stable printing quality and contributing to the development of 3D printing. The systematic organization and design presented in this study provide valuable reference for future extrusion system developers on how to adjust the parameters of each component to achieve the desired goals when dealing with different material properties. Through experimentation, it was observed that the extrusion system could be driven with minimal power when the dimensions of the extrusion head were set to 8 cm (length), 2.5 cm (width), and 5 cm (height), and when the blade spacing was segmented into four sections and the blade angle was set to 76 degrees, resulting in successful extrusion operations.**

***Keywords*—continuous helical blades, extrusion systems, 3D printing technology, parametric design**

I. Introduction

In recent years, due to the rapid development in the field of extrusion printing, 3D printing technology has become a crucial area in the manufacturing industry. The diverse demands for different printing materials and end products have contributed to the increasing importance of 3D printing technology. The applications of various printing materials have become increasingly diversified. Generally, 3D printing equipment consists of two major components: the frame system, which controls the position of the extrusion head during printing, and the extrusion system, which handles the printing materials. The current variety of extrusion system designs [1, 2] is a response to the different material characteristics, and the stacking methods for printing using different materials also vary [3]. The complexity of extrusion system designs arises from the lack of a comprehensive analysis and organization of these systems. The goal of this study is to conduct a thorough analysis and organization of the extrusion system, enabling the use of a single set of equipment to be compatible with different materials and even variations in the final printed products. By systematically analyzing the mechanical performance of different materials in extrusion systems with various parameter settings [4], suitable parameter configurations for different material properties can be identified, leading to the discovery of the most efficient combinations. Consequently, once the material properties are determined, the extrusion system can be adjusted accordingly by modifying the parameters of its components to accommodate the differences in material properties. This approach enables the development of an extrusion system that can adapt to all material properties, making the printing process easier for all types of materials.

A. Flow Chart (see Fig. 1)

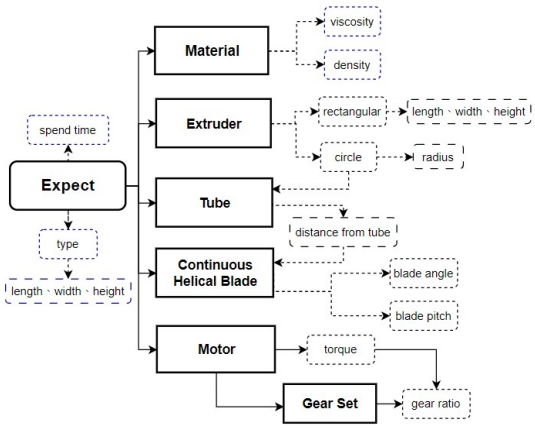

Fig. 1. Flow chart.

B. Mechanism Exploded Diagram (see Fig. 2)

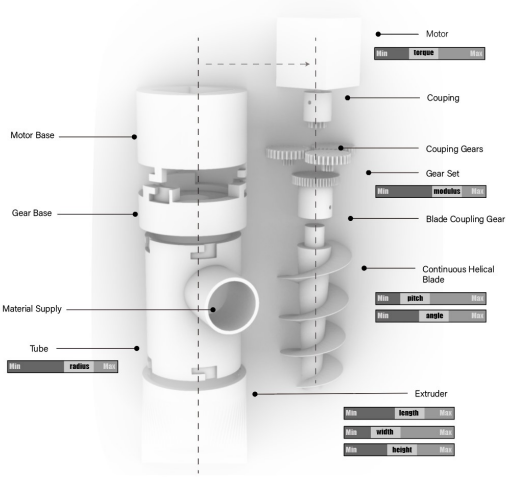

Fig. 2. Mechanism exploded diagram.

C. Framework

The extrusion system can be divided into two main components: the primary process and the minor branches. The primary process primarily consists of components comprising the extrusion mechanism, while variations in the parameters of these components can influence the minor branches. The design sequence of the primary process is determined by the order of mechanical design. Firstly, it is essential to determine the desired pattern of the final product and select the appropriate materials, while understanding their properties, such as viscosity and density. Subsequently, based on the material properties and the requirements of the final product, the dimensions of the extrusion head, including its length, width, and height, are determined. Since the source area of the extrusion head is equivalent to the cross-sectional area of the extrusion tube, the sizing of the extrusion tube is achieved upon completion of the extrusion head configuration. Next, considering the initial extrusion settings, the spacing between consecutive helical blades and the angle of the blades are determined. Ultimately, upon finalizing all extrusion components, the required magnitude of motor torque can be calculated, enabling the selection of an appropriate motor specification to complete the configuration of the entire extrusion system.

II. Research Methodology

A. Flow Simulation

Upon completing the mechanical design of the extrusion system, in order to gain preliminary insights into the operational performance of the system under different parameters and to understand the internal state during the extrusion process, this study utilizes SOLIDWORKS Flow Simulation for simulation testing. This approach allows for the acquisition of various mechanical values of the extrusion system during operation, facilitating improvements in the mechanical design aspect.

1) Comparative analysis of different materials' simulations

Simulations were conducted for four different materials: slurry, water, apple sauce, and olive oil. Among them, water is a Newtonian fluid, while slurry, apple sauce, and olive oil are non-Newtonian fluids. The objective was to understand the differences between Newtonian and non-Newtonian fluids in the context of extrusion experiments and compare the variations observed among different non-Newtonian fluids during the extrusion process.

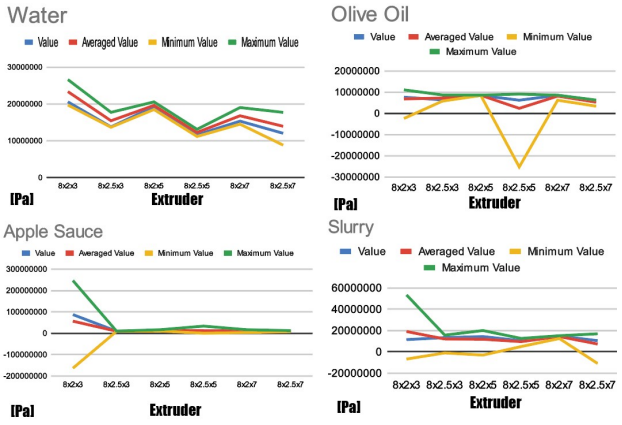

Fig. 3. Impact on the overall pressure with varying extrusion head parameters.

In the case of Newtonian fluid material like water (Fig. 3), it is evident that increasing the height of the extrusion head results in a relatively lower total pressure. Similarly, widening the extrusion head also leads to a relatively lower total pressure. For non-Newtonian fluids such as slurry (Fig. 3), the results exhibit slight similarities to water. Generally, higher heights and wider widths of the extrusion head result in a relatively lower total pressure. However, for non-Newtonian fluids like apple sauce (Fig. 3) and olive oil (Fig. 3), only the 8×2×3 extrusion head configuration demonstrates a more pronounced increase in total pressure. In other parameter settings, there is minimal impact on the maximum total pressure.

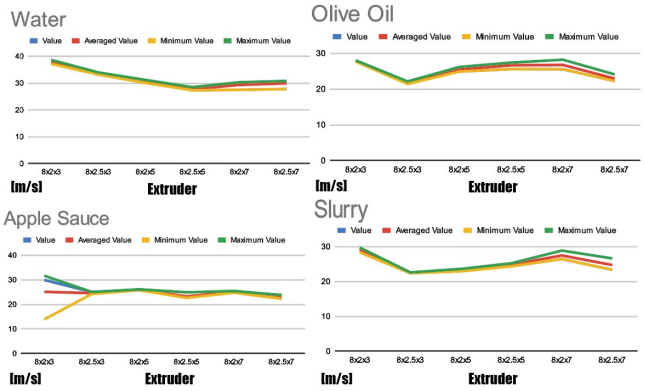

Fig. 4. Influence on the average velocity with different extrusion head parameters.

Regarding the Newtonian fluid material, water (Fig. 4.), it can be observed that in the extrusion outlet, a smaller area results in relatively higher velocity, with the minimum velocity achieved in the 8×2.5×5 extrusion head configuration. This suggests a U-shaped relationship between velocity and outlet area. For non-Newtonian fluids, both slurry (Fig. 4) and olive oil (Fig. 4) exhibit similar results. In the 3 and 7 height extrusion heads, smaller areas correspond to relatively higher velocities. Lastly, in the case of apple sauce (Fig. 4), a similar trend can be observed between velocity and pressure performance, indicating a proportional relationship between velocity and pressure in the apple sauce material.

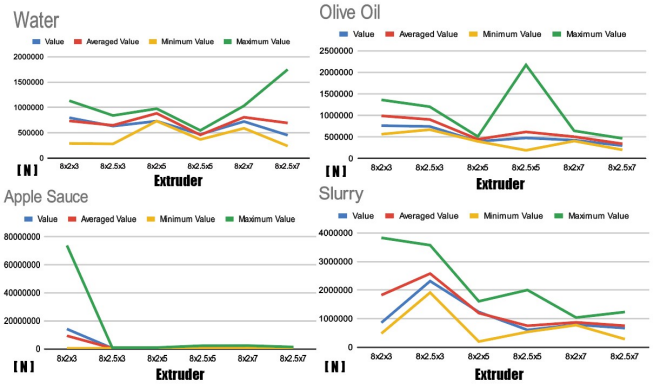

Fig. 5. Impact of the force exerted by different extrusion head parameters.

Regarding the Newtonian fluid material, water (Fig. 5), excluding the 8×2.5×7 extrusion head parameter, the following generalizations can be made: as the height increases, the force decreases relatively, and widening the extrusion head also leads to a relatively lower force, demonstrating a similar relationship as the total pressure. For the non-Newtonian fluid, slurry (Fig. 5), it is observed that

the force exhibits a relationship with the height of the extrusion head. As for olive oil (Fig. 5), apart from the extreme value in the 8x2.5x5 configuration, the curve shows that as the height increases, the force tends to decrease relatively. Lastly, in the case of apple sauce (Fig. 5), a similar trend can be observed between force, pressure, and velocity, indicating a proportional relationship between force, velocity, and pressure in the apple sauce material.

2) Simulation of pressure in the extrusion system

After conducting preliminary analysis on the four different materials, there is a particular interest in the slurry material. Therefore, further simulations were conducted to gain a deeper understanding of slurry. With a continuous helical blade rotation speed of 50 rad/s and a feed rate of 1 m^3/s at the inlet, a comparison of material contact surface pressures was performed for different extrusion outlets.

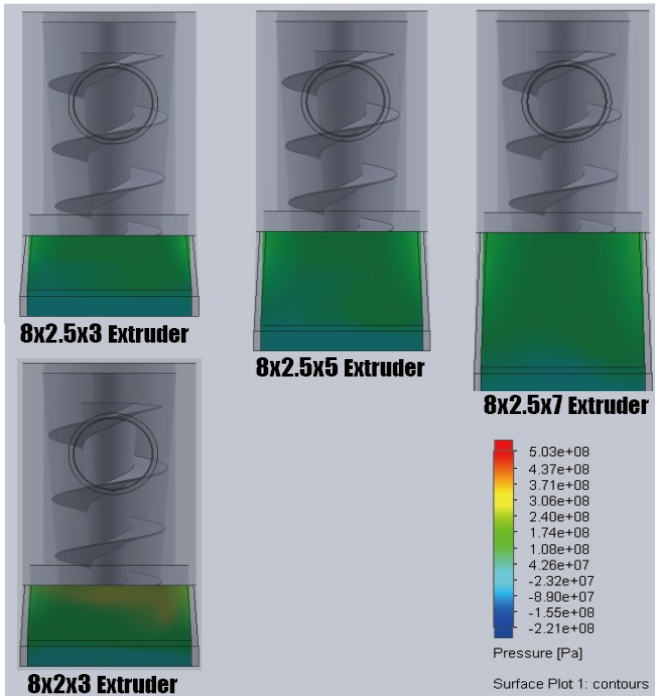

Fig. 6. Extrusion system.

From Fig. 6, it can be observed that the height of the extrusion head does not have a significant impact on the pressure variation at the extrusion head. However, it can be observed that the width of the extrusion head has a notable influence on the pressure at the extrusion head.

3) Simulation of flow velocity in the extrusion system

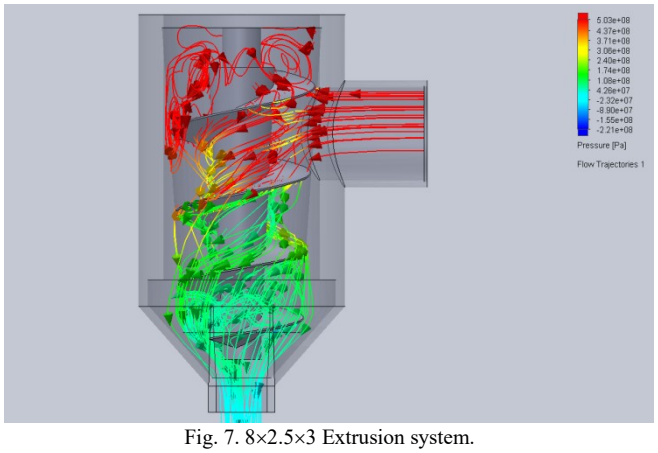

Fig. 7. 8×2.5×3 Extrusion system.

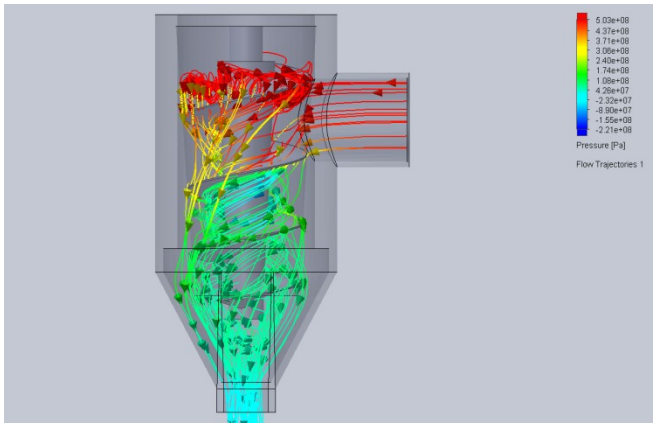

Fig. 8. 8×2.5×5 extrusion system.

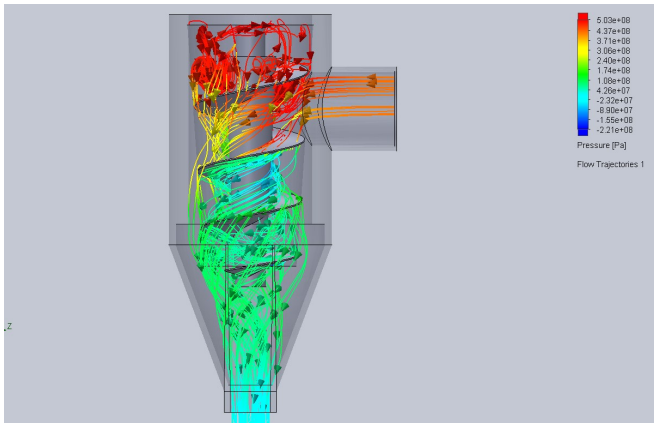

Fig. 9. 8×2.5×7 extrusion system.

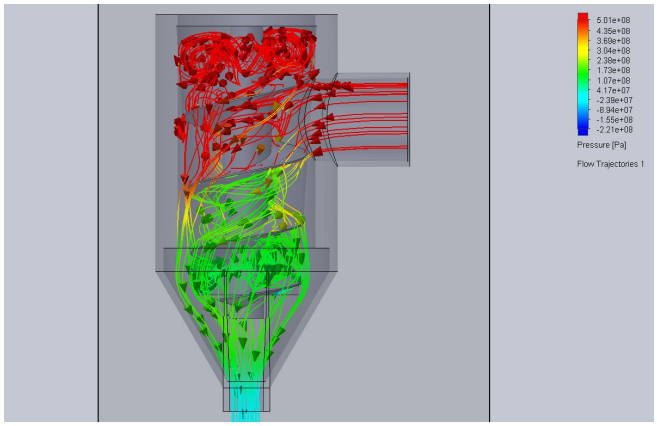

Fig. 10. 8×2×5 extrusion system.

From Figs. 7–9, it is evident that the height of the extrusion head has a significant influence on the flow velocity. Furthermore, from (Fig. 9) and (Fig. 10), it can be observed that the width of the extrusion head also has a notable impact on the flow velocity within the extrusion system under the same conditions.

B. Material - Clay

Following that, clay was selected as the material with properties similar to slurry for the experimental measurements. In this study, clay was chosen to undergo a series of tests not only because of its similarity to slurry but also due to its soft and malleable nature, allowing for easy cutting, shaping, or molding into various forms. Additionally, clay is a natural material that is relatively environmentally friendly compared to other materials. Clay, as the experimental material, offers advantages such as high workability, thermal stability, and chemical stability, making

it suitable for this experiment and research.

C. Sensor - Force-Sensing Resistor (FSR)

In order to quantify the differences observed under various parameters for the final extrusion system, a motor was chosen as the power source. A manual version of the extrusion system was specifically designed, with the motor power end transformed into a handle. Additionally, an FSR (force-sensitive resistor) pressure sensor was installed on the grip of the handle to quantitatively measure the required force in the tangent direction of force application. The pressure sensor exhibits different curves of force sensing when different pull-up resistor values are used. For this experiment, a 51k-ohm resistor was ultimately chosen as the pull-up resistor. Weight differences of 200 grams were used to measure the values obtained by the pressure sensor, resulting in the relationship graph (Fig. 11) as follows.

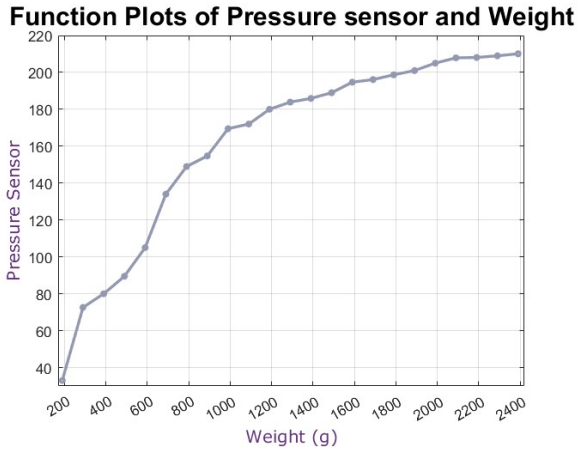

Fig. 11. Pressure sensor and weight diagram.

D. Extruder

After determining the material, the testing of the extrusion head was conducted. Following the flow simulation, a fixed circular source area of 25.16 square centimeters was chosen, and the width of the rectangular extrusion end was varied between 2.5 centimeters and 2 centimeters. As a result, there are two different areas at the extrusion end: 14.1504 square centimeters and 10.5391 square centimeters. The distance between the circular area and the rectangle (referred to as "height") was set at 3 centimeters, 5 centimeters, and 7 centimeters. The behavior of extrusion was observed in six different combinations where the source area was greater than the extrusion end area. However, during the clay extrusion test using the 8×2.5×3 extrusion head, the clay was unable to completely fill the space inside the extrusion head. Therefore, when discussing the results, consideration will be given to using data references specifically for this extrusion head (see Table 1 and Fig. 12).

Table 1. Extrusion head parameters

Extrusion Head	**1**	**2**	**3**
Length × Width × Height	8×2.5×7	8×2.5×5	8×2.5×3
Area	14.1504	14.1504	14.1504
Full or Not	o	o	×
Extrusion Head	4	5	6
Length × Width × Height	8×2×7	8×2×5	8×2×3
Area	10.5391	10.5391	10.5391
Full or Not	o	o	o

Fig. 12. Model of the extrusion head.

Table 2. Extrusion head pressure detection value

Extrusion Head	**8×2×3**			**8×2.5×3**			**8×2×5**			**8×2.5×5**			**8×2×7**			**8×2.5×7**		
1	228	231	210	195	210	193	225	255	262	135	179	166	200	166	159	182	160	122
2	232	228	220	200	230	227	235	293	229	144	198	162	205	189	182	208	243	145
3	238	227	213	208	239	207	240	320	226	151	203	171	205	204	214	220	221	161
4	216	216	219	190	245	211	254	298	254	174	205	161	206	192	246	231	252	143
5	192	262	206	193	252	194	190	307	242	176	209	220	268	213	269	227	242	188
6	190	207	223	161	242	210	170	321	299	200	261	223	226	216	268	222	265	189
7	170	191	216	161	200	217	181	326	216	210	228	233	218	215	262	265	252	160
8	173	191	256	219	208	212	165	270	189	209	224	238	221	197	231	227	259	241
9	178	187	277	225	189	218	190	319	188	210	217	240	241	219	223	263	244	197
10	151	174	267	174	207	203	174	294	193	228	193	238	250	192	221	185	230	177
11	174	174	187	163	152	199	183	351	161	188	188	243	244	234	227	215	205	175
12	149	178	108				181	251	151	187	196	188	213	224	226	217	189	163
13							171	208	145	201	210	167	243	244	227	226	202	154
14										198	209	165	220	221	214	202	191	169
15						190	179	165	185	164	228	15						
16							175	163	222			16						

Initially, the dimensions of the extrusion head were set as the manipulated variables, with length, width, and height being considered. The blade angle (86 degrees) and blade spacing (3.5 revolutions) were designated as the control variables. Using the manual version of the extrusion system, six extrusion operations were conducted with the same experimental setup, repeated three times. The recorded values detected by the pressure sensor were documented in Table 2. The highest recorded value was regarded as the maximum static friction force. The three recorded values were averaged to obtain the average maximum static friction force. Subsequently, the obtained values for the maximum static friction force were averaged to calculate the average dynamic friction force. The three recorded values were also averaged to determine the average dynamic friction force.

The line graph Fig. 13 depicting the average maximum static friction force and average dynamic friction force reveals that the dimensions of the extrusion head, namely length, width, and height, exhibit relatively lower values for the 8×2.5×5 configuration.

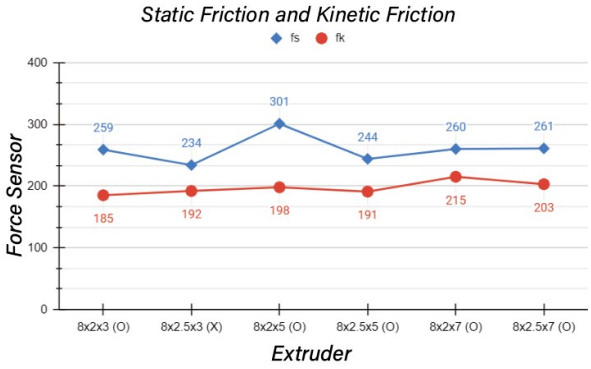

Fig. 13. The average maximum static friction and dynamic friction of the extrusion head experiment.

E. Continuous Helical Blade

The continuous helical blades play a crucial role in the extrusion system, and the choice of blade configuration has a significant impact on the extrusion outcome [5, 6]. In this study, the parameter variations of the continuous helical blades are divided into two aspects. The first parameter involves adjusting the blade spacing, with four different blade quantities: 3, 3.5, 4, and 5, within the same distance. The aim is to investigate the effects of these four blade spacings on the extrusion process. The second parameter involves altering the blade angle while keeping the blade spacing constant. The four different blade angles tested are 66°, 76°, 86°, and 96°, aiming to examine their impact on the extrusion process (see Fig. 14).

Fig. 14. Model of continuous helical blade.

Initially, the blade spacing is set as the manipulated variable, while the blade angle (86°) and the extrusion head (8×2×5) are kept as controlled variables. Using a manual version of the extrusion system, the extrusion process is performed with four different continuous helical blade configurations. The experiment is repeated five times, and the values detected by the pressure sensor are recorded (Fig. 15). The highest detected value is considered as the maximum static friction force. Taking the average of the five recorded values, the average maximum static friction force is obtained. Subsequently, the obtained values of the maximum static friction force are averaged, yielding the dynamic friction force. The average of the five recorded values is taken to obtain the average maximum dynamic friction force.

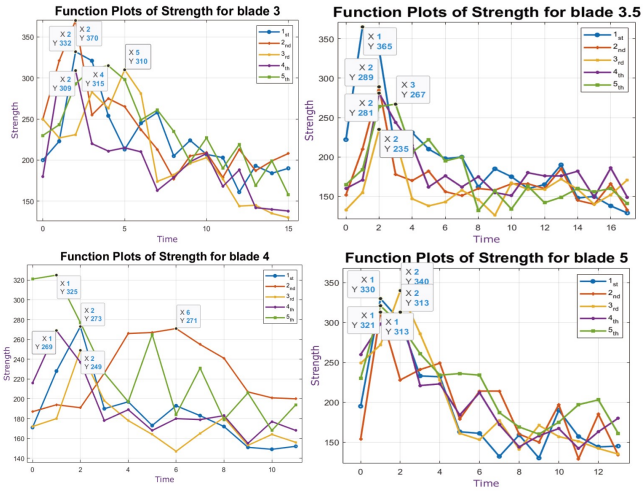

Fig. 15. Function plots of strength with different spacing of continuous helical blades.

The average maximum static friction force and average dynamic friction force obtained in the experiment are plotted on a line graph (Fig. 16.). It can be observed that the parameter of a blade spacing of 4 for the continuous spiral blades corresponds to a relatively smaller value of the maximum static friction force.

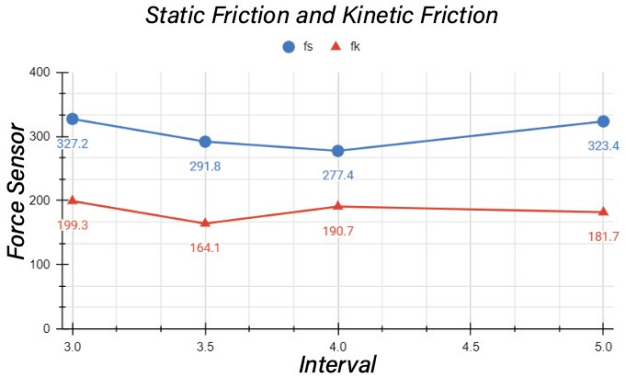

Fig. 16. The average maximum static friction and dynamic friction of continuous helical blade interval change.

The blade angle of the continuous spiral blades is now set as the manipulated variable, while the blade spacing (3.5) and the extrusion head (8×2×5) are kept as controlled variables. Using the manual version of the extrusion system, four different continuous spiral blades are tested. The experiment is conducted five times, and the values detected by the pressure sensor are recorded (Fig. 17). The highest detected value is considered as the maximum static friction force, and the average of the five values is calculated to obtain the average maximum static friction force. Subsequently, the obtained values of the maximum static friction force are averaged to determine the dynamic friction force, and the

average of the five values is taken as the average maximum dynamic friction force.

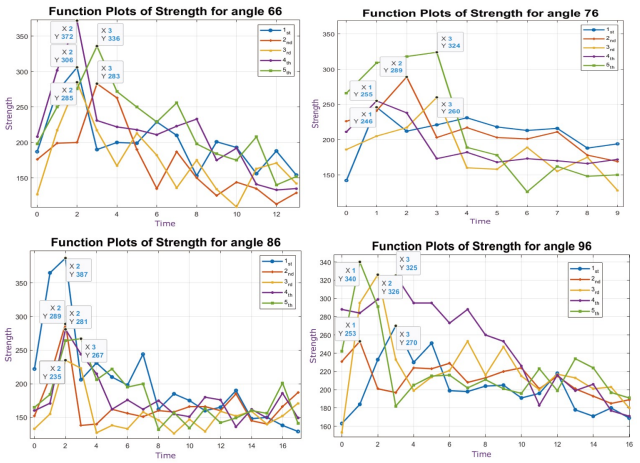

Fig. 17. Function plots of strength with different angle of continuous helical blades.

For the obtained average maximum static friction force and average dynamic friction force, a line graph (Fig. 18) is plotted. It can be observed that under the parameter of a blade angle of 76 degrees for the continuous spiral blades, there is a relatively smaller value for the maximum static friction force.

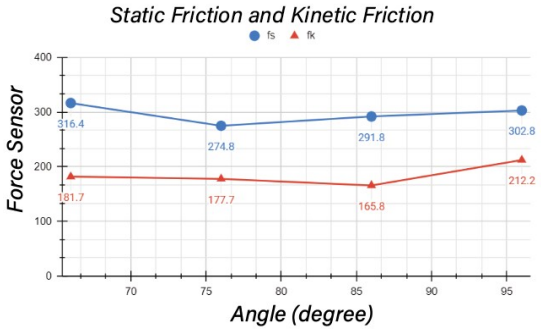

Fig. 18. The average maximum static friction and dynamic friction of continuous helical blade angle change.

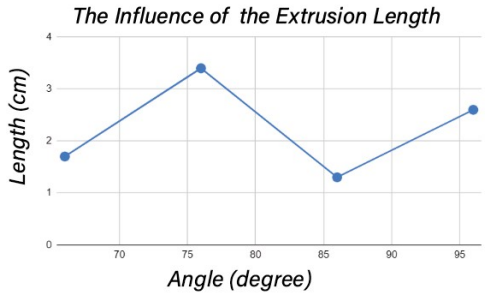

Fig. 19. The influence of the number of blades on the extrusion length.

Furthermore, this study aims to investigate the effect of the number of blades on the applied force as well as the extrusion length. With the blade angle (86 degrees) and extrusion head (8×2×5) kept constant, the extrusion action is performed for four different blade spacing values. Starting from a fixed point, the manual version of the extrusion system is rotated, completing two full revolutions. The goal is to observe the relationship between blade spacing and the length of the extruded material. The resulting relationship (Fig. 19) reveals an inverse proportion between the number of blades and the blade spacing. Therefore, as the number of blades decreases and the blade spacing increases, a greater amount of clay can be pushed through the system.

Moreover, this study aims to investigate the influence of blade angle on both the applied force and extrusion length. Similarly, with the blade spacing (3.5) and extrusion head (8×2×5) set as control variables, the study conducts extrusion operations for four different blade angles. Starting from a fixed point, the manual extrusion system is rotated for two complete revolutions with consistent handling. The objective is to observe the relationship between blade angle and extrusion material length. The resulting relationship (Fig. 20) reveals that a blade angle of 75 degrees exhibits the most favorable correlation between frictional force and clay propulsion.

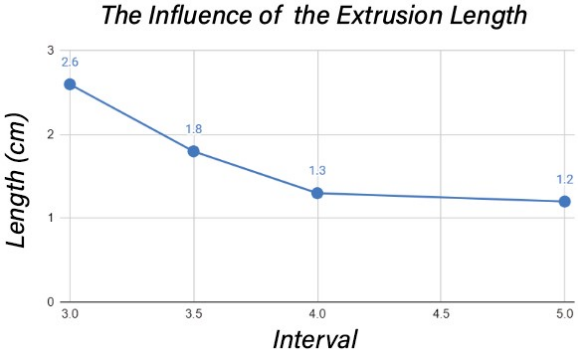

Fig. 20. Effect of number of blades on extrusion length.

III. Result

The results obtained from the actual experiments are summarized and compared with the findings of the SOLIDWORKS Flow Simulation analysis. The results can be classified into four main categories:

- Influence of motor: This category includes the rotational speed of the spiral blades affected by the motor and the speed of material extrusion.
- Parameters of continuous spiral blades: This category encompasses the effects of blade spacing, blade angle, and the gap between the spiral blades and the pipe wall.
- Parameters of the circular pipe: This category involves the impact of pipe diameter, pipe length, and the increased area of the circular end (A1).
- Parameters of the extrusion head: This category considers the influence of the average cross-sectional area and the area of the rectangular end on the extrusion process.

By organizing the results according to these four categories, a comprehensive understanding of the experimental and simulated findings can be achieved (see Table 3).

Table 3. Extrusion system parameter comparison

	Extrusion System
Motor	The rotational speed of the helical blades decelerates. Diminish the velocity, v2, of the rectangular end.
Continuous Helical Blade	Reduce the spacing of the helical blades. Increase the angle of the helical blades. Reduce the gap between the helical blades and the pipe wall.
Tube	Increase the diameter of the pipe. Shorten the length of the pipe. Enlarge the area, A1, of the circular end.
Extruder	Reduce the average cross-sectional area. Decrease the area, A2, of the rectangular end.

The relationships described above are based on situations where lower force is desired (smaller rotational torque). However, if the focus is not primarily on force magnitude or rotational torque, other prioritized considerations can be based on extrusion speed (fluid velocity) or extrusion volume (size of multiple outlets).

Fig. 21. Extrusion experiment (8×2.5×5) and (8×2×7).

In the final stage, extrusion tests were conducted on the extrusion system using clay as the material (Fig. 21) Different parameter settings for the extrusion head and continuous helical blades were tested, and they were able to achieve the desired objectives set for each configuration. The system demonstrated its capability to adapt to various parameter combinations, enabling successful extrusion of clay material.

IV. Conclusion

In conclusion, this study addressed the adaptability issues of extrusion systems for various materials and proposed a systematic organization method. By adjusting the parameters of the extrusion system components, the study aimed to enhance the stable printing quality of the system for different material properties. It was found that the extrusion system could be driven with minimal power when the dimensions of the extrusion head were set to 8 cm (length), 2.5 cm (width), and 5 cm (height). Furthermore, by utilizing continuous helical blades to assist with material discharge, the extrusion efficiency of the system was improved, leading to further enhancement in printing quality stability. Specifically, when the blade spacing was segmented into four sections and the blade angle was set to 76 degrees, the extrusion system could be driven with minimal power to successfully complete the extrusion process.

V. Future Research

The primary methodology employed in this study revolves around the adjustment of the extrusion system's parameters, such as the length, width, and height of the extrusion head, the spacing between the continuous helical blades, and the angle of the blades. These adjustments allow for the calculation of the required motor torque, facilitating the completion of the entire extrusion system's component design. During experimentation, the utilization of continuous helical blades for material extrusion proves instrumental in enhancing both the stability and quality of the extrusion process. By systematically organizing and designing the parameters within the extrusion head system, this study provides valuable insights for future reference in 3D printing applications, specifically concerning the selection of extrusion heads for different material characteristics. This enables the adaptation of various component parameters to achieve predetermined objectives. It is worth noting, however, that this study does not delve into the substantial impact of different materials on the extrusion system. Consequently, further experimentation and research are necessary to validate the feasibility and efficacy of the proposed methodology and its results. The systematic design approach for the extrusion system and the application of continuous helical blades presented in this study hold significant value and potential for future developments. Nonetheless, additional research and experimentation are still required to ensure their feasibility and effectiveness.

Conflict of Interest

The authors declare no conflict of interest.

Author Contributions

The responsibilities of the Huai-Chi Tsai include independently carrying out data collection, experimental design, conducting experiments, data analysis, and writing the paper. Pei-Hsien Hsu proposed the topic of the paper and provided the initial framework; all authors had approved the final version.

Acknowledgment

The authors wish to thank Hsin.

References

[1] E. R. Ruszuk *et al*., "3D printing ceramics — Materials for direct extrusion process," *Ceramics*, vol. 6, no. 1, pp. 364–385, 2023.

[2] A. Ruscitti *et al*., "A review on additive manufacturing of ceramic materials based on extrusion processes of clay pastes," *Ceramica*, vol. 66, no. 380, pp. 354–366, 2020.

[3] B. Perez *et al*., "Impact of macronutrients printability and 3D-printer," *Food Chemistry*, vol. 287, pp. 249–257 2019.

[4] K. D. Bouzakis *et al*., "Experimental and FEM-supported investigation of wet ceramic clay extrusion for the determination of stress distributions on the applied tools' surfaces," *Journal of the European Ceramic Society*, vol. 28, no. 11, pp. 2117–2127, 2018.

[5] C. Marschik *et al*., "Melt conveying in single-screw extruders: Modeling and simulation," *Polymers*, vol. 14, no. 5, 2022.

[6] M. Robinson and P. W. Cleary, "Flow and mixing performance in helical ribbon mixers," *Chemical Engineering Science*, vol. 84, pp. 382–398, 2012.